Published in final edited form as:
Clin Cancer Res. 2005 May 15; 11(10): 3743. doi:10.1158/1078-0432.CCR-04-1990.

Functionality of Androgen Receptor–Based Gene Expression Imaging in Hormone Refractory Prostate Cancer

Makoto Sato[1], **Mai Johnson**[1,2], **Liqun Zhang**[3], **Sanjiv S. Gambhir**[4,5,6,7], **Michael Carey**[3,5,6], and **Lily Wu**[1,4,5,6]

[1]Department of Urology, David Geffen School of Medicine, University of California, Los Angeles, Los Angeles, California

[2]Department of Molecular Cellular and Integrative Physiology, David Geffen School of Medicine, University of California, Los Angeles, Los Angeles, California

[3]Department of Biological Chemistry, David Geffen School of Medicine, University of California, Los Angeles, Los Angeles, California

[4]Department of Molecular and Medical Pharmacology, David Geffen School of Medicine, University of California, Los Angeles, Los Angeles, California

[5]Crump Institute for Molecular Imaging, David Geffen School of Medicine, University of California, Los Angeles, Los Angeles, California

[6]Jonsson Comprehensive Cancer Center, David Geffen School of Medicine, University of California, Los Angeles, Los Angeles, California

[7]Department of Radiology and the Bio-X Program, Stanford University, Stanford, California

Abstract

Purpose—A highly augmented, prostate-specific two-step transcriptional amplification (TSTA) method was developed with the ultimate goal of delivering an effective and safe gene-based treatment to prostate cancer patients. Because very limited treatment options are available for recurrent hormone refractory prostate cancer (HRPC), it is imperative to assess whether the prostate-specific antigen (PSA) promoter-based TSTA gene therapy will be functional in HRPC.

Experimental Design—We tested the TSTA-driven adenovirus vector on three androgen-dependent and six HRPC models. Real-time gene expression was monitored by both optical imaging and the combined modality of positron emission tomography (PET) and computed tomography.

Results—The TSTA-driven firefly luciferase expressing adenoviral vector was active in all androgen receptor (AR)–expressing HRPC models, but inactive in AR- and PSA-negative lines. Interestingly, the TSTA-mediated gene expression was induced by hydrocortisone in MDA PCa 2b, a cell line with mutated AR that possesses altered ligand specificity. In animal models, the TSTA-mediated optical signal was more robust in the HRPC than androgen-dependent tumors. In a parallel trend, a TSTA vector that expresses the herpes simplex virus thymidine kinase PET reporter gene also displayed more robust PET signal in the HRPC tumor.

Conclusions—The activity of TSTA system is AR dependent and it recapitulates the functional status of endogenous AR. These data support the conclusion that AR function is activated in HRPC despite castrated levels of androgen. Together with the fact that majority of recurrent prostate cancers

Requests for reprints: Lily Wu, Department of Urology, University of California, Los Angeles, 675 Charles Young Drive South, Los Angeles, CA 90095-1738. Phone: 310-794-4390; Fax: 310-825-3027; lwu@mednet.ucla.edu..

express AR and PSA, we foresee that the TSTA approach can be a promising gene therapy strategy for the advanced stages of prostate cancer.

Although recent data suggest that the death rate from prostate cancer is decreasing by 4% per year since 1994, it is still the second leading cause of cancer death in men, with an estimated 230,110 new cases and 29,900 deaths in the United States in 2004 (1). About one third of men with prostate cancer believed to have localized disease will already have micrometastasis at the time of therapy (2). Despite treatment with surgery, 20% to 30% of the patients will suffer from disease recurrence as defined by serum prostate-specific antigen (PSA) elevation (3,4). In the aggressive, high-grade (Gleason 8-10) disease, majority of PSA recurrence is detected within 2 years after surgery with median survival of <3 years (3). Hormone therapy blocking androgen function can induce short-term remission, but the refractory disease eventually recurs (2). At this stage, the disease is defined as androgen-independent (AI) or hormone refractory prostate cancer (HRPC). The median survival for patients with metastatic HRPC is ~18 months, and systemic chemotherapy provides only a palliation of symptoms (5).

Androgen receptor (AR), the mediator of the physiologic effects of androgen (6), regulates the growth of normal and malignant prostate epithelial cells. Following the binding of the activating ligand dihydrotestosterone, AR translocates from the cytoplasm into the nucleus, binds directly to DNA recognition sites, and induces the expression of androgen-responsive genes, including *PSA*. A central issue in HRPC is to understand the role of AR in this stage of disease. Would AR function be obsolete under treatment where the activating ligand was depleted? Several mechanisms have indicated the continual involvement of AR in HRPC (reviewed in ref. 7), including (*a*) AR gene amplification and overexpression; (*b*) altered ligand specificity of AR (promiscuous AR); and (*c*) activation of AR through crosstalks with other AI pathways. The precise role of AR in clinical situations is not fully understood. However, given the fact that AR expression is documented in the majority of HRPC cases (8,9) and that PSA remains the most reliable marker for recurrent, metastatic prostate cancer (10), it is highly probable that the gene regulatory activity of AR is functional in this setting.

Several PSA or probasin promoter-based gene therapy approaches have been developed (ref. 11; reviewed in ref. 12). However, thorough investigations questioning the functionality of these AR-dependent therapeutic strategies in HRPC have not been completed. The current report uses cell-based activity measurements and *in vivo* molecular imaging to show that a highly amplified PSA promoter-derived (two-step transcriptional amplification, TSTA) system is active in HRPC models. Noninvasive bioluminescence imaging and positron emission tomography (PET) illustrate that the prostate-specific TSTA gene expression vectors exhibit robust activity in HRPC as well as androgen-dependent (AD) tumors. We project that our vector-based gene therapy coupled to molecular imaging would be a promising therapeutic option to develop for treating patients with recurrent disease.

Materials and Methods

Adenovirus constructs

AdTSTA-FL was constructed as previously described (13,14). The AdTSTA-sr39tk was constructed with the AdEasy system (15). The head-to-head orientation of activator (BCVP2) and reporter (SR39tk) in the single plasmid was constructed by replacing FL with SR39tk in PBCVP2G5-L (16). The BCVP2G5-sr39tk fragment generated by *Not*I and *Sal*I digestion of PBCVP2G5-sr39tk was inserted into pShuttle, which was used in bacterial recombination to generate the full-length virus. The virus was grown on 293 cells, purified on a CsCl gradient, and titered by plaque formation assays on 293 monolayers. The level of replication competent adenovirus contamination in the viral stocks was evaluated by plaque formation on A549 cells.

No plaque was detected at 10^8-fold higher viral stock dilution compared with assays on 293 cells.

Prostate cell lines and luciferase activity assay

The human prostate cancer cell lines LNCaP, CWR22Rv1, DU145, and PC-3 were grown in RPMI 1640 supplemented with 10% fetal bovine serum. Iscove's modified DMEM was used for LAPC-4. MDA PCa 2b line obtained from American Type Culture Collection (Manassas, VA) was grown in BRFF-HPC1 (Athena Environmental Sciences, Baltimore, MD) supplemented with 20% fetal bovine serum. For AdTSTA-FL assays, the cultured cells were plated onto 24-well plates at 5×10^4 cells per well with phenol red–free RPMI 1640 supplemented with 10% charcoal-stripped fetal bovine serum. Cells were counted and infected at 1 plaque-forming unit per cell [multiplicity of infection (MOI) = 1]. At 48 hours postinfection, the cells were harvested and lysed in radioimmunoprecipitation assay buffer [1% NP40, 0.1% sodium deoxycholate, 150 mmol/L NaCl, 50 mmol/L Tris-HCl (pH 7.5), and 1 mmol/L phenylmethylsulfonyl fluoride]. Luciferase activity was measured according to the manufacturer's instructions (Promega, Madison, WI) using a luminometer (Berthold Detection Systems, Pforzheim, Germany). Each value was normalized with protein concentration and calculated as the average of triplicate samples. The infectivity of all cell lines was assessed by quantitative PCR of internalized viral DNA and expression mediated by constitutive AdCMV-FL as previously described (14). Relative to the infectivity of LNCaP cells (designated as 1), the infectivity of all other lines are within 2-fold. The highest infectivity was in CWR22rv1 (2.0) and the lowest was in PC-3 (0.7). Due to the similarity of infectivity among the cell lines, activity results reported here were not adjusted.

Synthetic androgen methylenetrienolone (R1881; NEN Life Science Products, Boston, MA) or the antiandrogen bicalutamide (casodex) was added to experiments as indicated. To measure the androgen induction effect, we used the activity in the presence of 10 μmol/L bicalutamide as the basal level rather than in charcoal-stripped fetal bovine serum. The TSTA system is highly amplified and low level of residual androgen in charcoal-stripped fetal bovine serum can activate expression (16). For Western analysis, cell lysates were fractionated on 4% to 20% gradient acrylamide gels (Bio-Rad, Hercules, CA) and subjected to immunoblot analysis with anti-AR N-20 (Santa Cruz Biotechnologies, Santa Cruz, CA) or β-actin A5316 (Sigma, St. Louis, MO) antibodies, and visualized with HRP-labeled secondary antibody and ECL (Amersham, Piscataway, NJ).

Statistical analyses were done using the two-tailed Student's *t* test. For all analyses, $P < 0.01$ was considered statistically significant.

Preparation of tumor cell suspension

Preparation of tumor cell suspensions was done by slight modification of a published protocol (17). Briefly, tumors were harvested, minced to 1 mm^3, and then incubated in 1% Pronase solution (Roche Molecular Biochemicals, Mannheim, Germany) for 20 minutes at room temperature. After overnight incubation in PrEGM media (Cambrex, Walkersville, MD) with Fungizone, the cultured cells were disaggregated by pipetting through sterile 200 μm Cell-Sieve mesh (Biodesign Inc. of New York, Carmel, NY). Tumor cells were infected at 1 plaque forming unit per viable cell (MOI = 1) and analyzed after 48 hours. No difference in the infectivity (determined by infection with a green fluorescent protein expressing adenoviral vector) or nonspecific viral toxicity was observed between the androgen-dependent and androgen-independent LAPC-9 tumor cells.

Thymidine kinase enzyme assay

LNCaP and LAPC-4 were plated onto six-well plates at 5×10^5 cells per well and infected with AdTSTA-sr39tk at MOI = 1. R1881 (10 nmol/L) or asodex (10 μmol/L) was added to the infected cells as indicated and the cells were harvested and lysed in 0.5% NP40, 25 mmol/L NaF, 3 mmol/L β-mercaptoethanol, and 10 mmol/L Tris-HCl (pH 7.0) after 48 hours. The protein concentration of the cell lysates was determined by the detergent-compatible protein assay (Bio-Rad); 1 μg of the lysate was mixed with 3 μL Tk mix ([^{3}H]penciclovir (Movarek Biochemicals, Brea, CA), 250 mmol/L Na_2HPO_4 (pH 6.0), 25 mmol/L ATP, and 25 mmol/L Mg acetate) and incubated at 37°C for 20 minutes. Reactions were terminated by the addition of 40 μL cold water and heating at 95°C for 2 minutes. Forty microliters of mixture was blotted onto DE81 filters (Whatman, Clifton, NJ). The filters were dried and washed thrice with 4 mmol/L ammonium formate and 10 μmol/L thymidine, once in water and twice in 95% ethanol. After drying, the filters were counted by scintillation. Each value was calculated as the average of duplicate samples.

Animal experiments with optical and positron emission tomography imaging

Animal care and procedures were done in accordance with the University of California Animal Research Committee guidelines. Ten- to twelve-week-old male SCID mice obtained from Taconic Farms (Germantown, NY) were implanted s.c. with a tumor chunk (~0.2 cm diameter) coated with Matrigel (Collaborative Research, Bedford, MA) and allowed to grow to ~0.8 cm diameter (18). For the optical imaging experiments, 10^7 plaque-forming units of AdTSTA-FL were subdivided and injected intratumorally (i.t.) into three sites. *In vivo* expression was monitored sequentially using a cooled IVIS CCD camera (Xenogen, Alameda, CA). For each imaging session, the mice were anesthetized with ketamine/xylazine (4:1), given the D-luciferin substrate (200 μL of 150 mg/kg substrate in PBS) i.p., and imaged after a 20-minute incubation. Images were analyzed with IGOR-PRO Living Image Software as described (13,19). Immunohistochemistry to detect AR expression in the tumor was done with anti-AR antibody (Upstate, Co., Charlottesville, VA) as previously described (13,19).

For micro-PET imaging, 10^9 plaque-forming units (~30 μL) of AdTSTA-sr39tk were injected i.t. for 4 consecutive days. PET imaging was done on day 7 using ~200 μCi [^{18}F]FHBG substrate (specific activity 5-10 Ci/mmol) that was administered via the tail vein. After 1 hour of uptake time, mice were given inhalation isoflurane anesthesia, placed in a prone position, and imaged for 20 minutes in the micro-PET scanner (Concorde Microsystems, Knoxville, TN). Images were reconstructed using a filtered back projection reconstruction algorithm. Micro–computed tomography (micro-CT; Imtek, Inc., Knoxville, TN) was done for the same animal sequentially, and images were overlapped using ASIPro VM (Concorde Microsystems).

Results

The transcriptional amplification activity in prostate cancer cell lines

We have developed several transcriptionally targeted gene expression systems based on the PSA gene regulatory regions. The method that exhibits most potent activity, tissue selectivity, and androgen regulation is termed two-step transcriptional activation. It uses an enhanced PSA promoter (20) that drives a potent GAL4VP16 synthetic activator, which in turn binds to tandem repeats of GAL4 binding sites to activate the secondary reporter or therapeutic gene. This TSTA method achieved nearly 1,000-fold augmentation of activity over the native PSA promoter and is more active than the strong viral cytomegalovirus promoter (14). Recently, we have shown that AR in hormone refractory LAPC-9 tumors is functionally active, and it binds to known sites in the PSA gene regulatory region by chromatin immunoprecipitation (13). Expanding upon this observation, the key objective of this study is to survey the activity

of TSTA vectors in a wider array of HRPC models and to visualize the *in vivo* activity of the vectors by multimodal molecular imaging techniques.

The activity of the TSTA adenoviral vector (AdTSTA-FL; Fig. 1A) was first determined in two AD lines LNCaP and LAPC-4, and three HRPC lines CWR22Rv1, DU145, and PC-3. As shown in Fig. 1B, AdTSTA-FL activity was negligible in the AR-negative DU145 and PC-3 lines. In the three AR-expressing lines, the activity of AdTSTA-FL was stimulated by androgen ranging from 11.4- to 60.6-fold. When bicalutamide (10 μmol/L) was given simultaneously in the presence of synthetic androgen R1881 (10 nmol/L), a ~50% suppression of peak activity was observed (data not shown). In the presence of androgen, LNCaP cells exhibited the highest expression at 4.8 times the level of LAPC-4 and 14.4 fold-higher than CWR22Rv1.

We also investigated the activation in a fourth HRPC line, MDA PCa 2b, which interestingly expresses AR with a double mutation (L701H and T877A) that allows gene expression and growth to become glucocorticoid responsive (21). As shown in Fig. 1C, gene expression mediated by this promiscuous AR responded to both androgen and hydrocortisone. The induction was 105-fold by hydrocortisone and 144-fold by R1881. The absolute expression level in MDA PCa 2b was 4.4-fold lower than CWR22Rv1. Based on these expression data, we deduced that the PSA-based TSTA method is active in HRPC but its activity is dictated by the AR function in the cell.

Two-step transcriptional amplification activity in hormone refractory LAPC-9 tumor monitored by optical imaging

LAPC-9 and LAPC-4 are two human prostate tumors that can recapitulate the clinical scenario of HRPC (17,18). They grow routinely in intact male mice and undergo tumor regression upon castration. However, after a substantial time delay, a hormone refractory tumor develops, mimicking the recurrence of HRPC. The activity of AdTSTA-FL was monitored by optical imaging of paired AD and hormone refractory LAPC-9 tumors from days 4 to 14 (Fig. 2A). By this real-time *in vivo* activity measurement, hormone refractory tumors supported a higher level of transgene expression than AD tumors. Immunohistochemistry analysis revealed that the AR protein was expressed in both AD and HRPC tumors, but the magnitude of expression is very heterogenous among the tumor cells (Fig. 2B).

Equivalent gene delivery into the different tumors by i.t. viral injection was difficult to achieve. Thus, we converted the paired tumors into single cell suspension to examine androgen regulation and the activity of the TSTA system more accurately. In doing so, the dosage of viral vector and androgen administered on a per cell basis can be controlled. The dispersed tumor cells were infected with AdTSTA-FL in the presence of specified ligands. AR protein and androgen-responsive FL activity was observed in both cell populations (Fig. 2C). In close agreement with the optical imaging results in tumors, we also observed that the activity of AdTSTA-FL is 7.2-fold higher in the hormone refractory (AI) than in AD tumor cells in culture in the presence of ≥1 nmol/L concentrations of R1881.

Use of the two-step transcriptional amplification vector in positron emission tomography imaging

It is important to develop molecular imaging approaches that can be applied in clinical settings for advanced prostate cancer. To this end, we adapted our prostate-specific gene imaging to PET, a radio-nuclide functional imaging modality that enables three-dimensional signal localization. An adenoviral vector that expresses the herpes simplex virus thymidine kinase (*HSV-tk*) PET reporter gene under the control of TSTA was generated (Fig. 3A). An enhanced HSV-tk variant, sr39tk, was incorporated into the AdTSTA-sr39tk because this variant *tk* gene augments the uptake of radiolabeled PET tracers and improves PET imaging sensitivity by 2-

fold (22). The sr39tk protein expression and enzymatic activity mediated by the vector was regulated by androgen (Fig. 3B and C).

AdTSTA-sr39tk was administered into AD and hormone refractory LAPC-4 tumors, and its activity was documented by the combined micro-PET/micro-CT. This combined imaging modality enables the precise localization of the PET signals with the anatomic information obtained from the CT scan. Using [^{18}F]FHBG as the PET substrate, robust signals were observed in both AD and hormone refractory LAPC-4 tumors (Fig. 3D). The activity was higher in the hormone refractory tumor (0.78% injected dose/g) than in the AD tumor (0.50% injected dose/g). These results confirm that the TSTA-mediated prostate-specific gene imaging is feasible for advanced stages of tumor using the clinically relevant PET.

Discussion

Effective treatment options for recurrent prostate cancer are notably limited. Our goal has been to develop novel gene-based diagnostic and therapeutic approaches to treat advanced stages of prostate cancer. Toward this end, the well-studied PSA promoter/enhancer was utilized to achieve prostate-specific gene expression. Given that transcriptional regulation of the PSA promoter/enhancer is AR dependent, it was prudent to first verify that our PSA promoter-based expression strategy is feasible in HRPC. In this study, we showed that the highly amplified prostate-specific TSTA gene delivery vectors are indeed functional in many models of HRPC under androgen-deprived conditions.

Our data support that the presence of functional AR is necessary to activate PSA-based promoter constructs. However, other factors are likely to modulate AR activity in HRPC cells. The 14-fold range of luciferase activity observed in different models does not correlate with the level of AR expression or the status of AR mutation in the cell lines. The AR in LAPC-4 is wild type, whereas it contains the T877A mutation in LNCaP and the H874Y mutation in the ligand-binding domain of CWR22Rv1. Differential activity of coactivators of the AR pathway could modulate AR function *in vivo*. Gregory et al. (23) reported elevated level of nuclear receptor coactivators, SRC1, and SRC2 in recurrent prostate cancer. Recently, Dr. Tindall's group also showed that coactivator p300 confers increased growth and progression potential in prostate cancer (24). Many other growth signaling pathways, such as IGF, Her2, or IL6, can also modulate AR-mediated expression (reviewed in ref. 7). Further investigations are needed to determine the precise AR activation mechanism in different cases of HRPC.

Both optical imaging and PET illustrated higher TSTA activity in the hormone refractory xenograft subline versus the parental AD tumor in two models. These findings endorse the idea that activation of AR function occurs despite the castrated level of androgen *in vivo*. A recent report by Chen et al. (25) showed that 3- to 5-fold elevated expression of AR is a cardinal distinguishing feature between paired AD and hormone refractory tumors. Their work also supports that AR overexpression can lead to HRPC. In fact, the two models reported here were assessed in the gene expression profiling study (25). Moreover, our results showed that the real-time assessment of AR functional activity in prostate tumors, including HRPC, can be accomplished by introducing TSTA adenoviral vectors into the tumor.

In contemplating future applications in clinical settings, we postulate that the TSTA gene expression strategy will be active in all PSA-positive prostate cancers, which include the recurrent metastatic disease. Previous histologic evaluations of clinical materials have detected AR and PSA expression in all stages of prostate cancer (8,26,27). Recent preliminary results (reported at Specialized Programs of Research Excellence meeting July 2004, Baltimore MD) indicated that AR expression is detected in metastatic lesions, albeit at heterogeneous level. A subtype of HRPC, the neuroendocrine prostate cancer, lacks AR and is associated with poor

prognosis (28,29). We anticipate any AR-dependent gene expression approach will be inactive in neuroendocrine tumor cells. However, solitary neuroendocrine tumors are rare as most neuroendocrine tumor cells exist in small foci interspersed within conventional AR- and PSA-positive prostate adenocarcinoma. If an AR-dependent toxic gene therapy was applied to a mixed lesion, then indirect tumoricidal effects can be transmitted to neuroendocrine tumor cells via conventional prostate cancer cells by bystander effects (12).

Linking molecular imaging to gene therapy is a favorable method to assess the performance of the intended treatment. In an earlier study, visualization of distant metastases of prostate tumor was accomplished by optical imaging mediated through the use of a modified PSA promoter-based adenoviral vector (19). Due to the inability of light energy to penetrate deep into tissues, bioluminescence imaging is not applicable in humans. Thus, to translate the above-mentioned promising findings to the clinics, the application of a high-energy clinically relevant modality, such as PET, is needed. However, the HSV-tk–based PET imaging is several orders of magnitude less sensitive than optical imaging in small animal studies (30). The nearly three-order gain in activity of TSTA over native PSA promoter is a key factor to achieve the successful PET imaging of HRPC. Because the same principles are at work in animal micro-PET as in clinical PET, this result supports the idea of an equivalent gene-based approach in clinical studies.

Many studies have shown that the *sr39tk* gene can function effectively both as a PET reporter gene as well as a toxic suicide gene (12,31). Recently, the AdTSTA-sr39tk was applied in a "one-two punch" imaging and suicide gene therapy to treat prostate tumor.[8] Compared to a constitutive cytomegalovirus-driven vector, the prostate-targeted TSTA vector not only elicited equivalent tumoricidal effects but also dramatically reduced systemic liver toxicity. The PET imaging correlated entirely with the therapeutic outcomes. These results indicate that the TSTA methodology is a promising platform to build gene-based diagnostic and therapeutic approaches to manage HRPC.

Acknowledgments

We thank W. Ladno, J. Edwards, and Dr. D. Stout for their skillful assistance in PET/CT imaging; Baohui Zhang for technical assistance; Giri Sulur for assistance on manuscript preparation; and Drs. David Agus (Department of Molecular and Medical Pharmacology, UCLA, Los Angeles, CA) and Margaret Black (Pharmaceutical Sciences, Washington State University, Pullman, WA) for the kind gifts of CWR22Rv1 cell line and polyclonal anti-tk antibody, respectively.

Grant support: Department of Defense grant DAMD17-03-1-0095 and NIH grant R01 CA101904 (L. Wu); Department of Defense grant DAMD PC 020177 (M. Carey); NIH grant R01 CA82214 and Small Animal Imaging Resource Program grant R24 CA92865 (S.S. Gambhir); an interdisciplinary grant from Jonsson Comprehensive Cancer Center (M. Carey, L. Wu, and S.S. Gambhir); and Department of Defense Congressionally Directed Medical Reseach Program postdoctoral fellowship, PC020531 (M. Sato).

References

1. Weir HK, Thun MJ, Hankey BF, et al. Annual report to the nation on the status of cancer, 1975-2000, featuring the uses of surveillance data for cancer prevention and control. J Natl Cancer Inst 2003;95:1276–99. [PubMed: 12953083]
2. Dowling AJ, Tannock IF. Systemic treatment for prostate cancer. Cancer Treat Rev 1998;24:283–301. [PubMed: 9805508]
3. Pound CR, Partin AW, Eisenberger MA, Chan DW, Pearson JD, Walsh PC. Natural history of progression after PSA elevation following radical prostatectomy. JAMA 1999;281:1591–7. [PubMed: 10235151]

[8]Johnson et al., submitted for publication.

4. Roehl KA, Han M, Ramos CG, Antenor JA, Catalona WJ. Cancer progression and survival rates following anatomical radical retropubic prostatectomy in 3,478 consecutive patients: long-term results. J Urol 2004;172:910–4. [PubMed: 15310996]
5. Tannock IF, deWit R, Berry WR, et al. TAX 327 Investigators. Docetaxel plus prednisone or mitoxantrone plus prednisone for advanced prostate cancer. N Engl J Med 2004;351:1502–12. [PubMed: 15470213]
6. Gelmann EP. Molecular biology of the androgen receptor. J Clin Oncol 2002;20:3001–15. [PubMed: 12089231]
7. Feldman BJ, Feldman D. The development of androgen-independent prostate cancer. Nat Rev Cancer 2001;1:34–45. [PubMed: 11900250]
8. Hobisch A, Culig Z, Radmayr C, et al. Distant metastases from prostatic carcinoma express androgen receptor protein. Cancer Res 1995;55:3068–72. [PubMed: 7541709]
9. Magi-Galluzzi C, Xu X, Hlatky L, et al. Heterogeneity of androgen receptor content in advanced prostate cancer. Mod Pathol 1997;10:839–45. [PubMed: 9267828]
10. Bok RA, Small EJ. Bloodborne biomolecular markers in prostate cancer development and progression. Nat Rev Cancer 2002;2:918–26. [PubMed: 12459730]
11. DeWeese TL, van der Poel H, Li S, et al. A phase I trial of CV706, a replication-competent, PSA selective oncolytic adenovirus, for the treatment of locally recurrent prostate cancer following radiation therapy. Cancer Res 2001;61:7464–72. [PubMed: 11606381]
12. Wu L, Sato M. Integrated, molecular engineering approaches to develop prostate cancer gene therapy. Curr Gene Ther 2003;3:452–67. [PubMed: 14529351]
13. Zhang L, Johnson M, Le KH, et al. Interrogating androgen receptor functionin recurrent prostate cancer. Cancer Res 2003;63:4552–60. [PubMed: 12907631]
14. Sato M, Johnson M, Zhang L, et al. Optimization of adenoviral vectors to direct highly amplified prostate-specific expression for imaging and gene therapy. Mol Ther 2003;8:726–37. [PubMed: 14599805]
15. He TC, Zhou S, da Costa LT, et al. A simplified system for generating recombinant adenoviruses. Proc Natl Acad Sci U S A 1998;95:2509–14. [PubMed: 9482916]
16. Zhang L, Adams JY, Billick E, et al. Molecular engineering of a two-step transcription amplification (TSTA) system for transgene delivery in prostate cancer. Mol Ther 2002;5:223–32. [PubMed: 11863411]
17. Craft N, Chhor C, Tran C, et al. Evidence for clonal outgrowth of androgen-independent prostate cancer cells from androgen-dependent tumors through a two-step process. Cancer Res 1999;59:5030–6. [PubMed: 10519419]
18. Klein KA, Reiter RE, Redula J, et al. Progression of metastatic human prostate cancer to androgen independence in immunodeficient SCID mice. Nat Med 1997;3:402–8. [PubMed: 9095173]
19. Adams JY, Johnson M, Sato M, et al. Visualization of advanced human prostate cancer lesions in living mice by a targeted gene transfer vector and optical imaging. Nat Med 2002;8:891–7. [PubMed: 12134144]
20. Wu L, Matherly J, Smallwood A, et al. Chimeric PSA enhancers exhibit augmented activity in prostate cancer gene therapy vectors. Gene Ther 2001;8:1416–26. [PubMed: 11571582]
21. Zhao XY, Malloy PJ, Krishnan AV, et al. Glucocorticoids can promote androgen-independent growth of prostate cancer cells through a mutated androgen receptor. Nat Med 2000;6:703–6. [PubMed: 10835690]
22. Gambhir SS, Bauer E, Black ME, et al. A mutant herpes simplex virus type 1 thymidine kinase reporter gene shows improved sensitivity for imaging reporter gene expression with positron emission tomography. Proc Natl Acad Sci U S A 2000;97:2785–90. [PubMed: 10716999]
23. Gregory CW, He B, Johnson RT, et al. A mechanism for androgen receptor-mediated prostate cancer recurrence after androgen deprivation therapy. Cancer Res 2001;61:4315–9. [PubMed: 11389051]
24. Debes JD, Sebo TJ, Lohse CM, et al. p300 in prostate cancer proliferation and progression. Cancer Res 2003;63:7638–40. [PubMed: 14633682]
25. Chen CD, Welsbie DS, Tran C, et al. Molecular determinants of resistance to antiandrogen therapy. Nat Med 2004;10:33–9. [PubMed: 14702632]

26. Sweat SD, Pacelli A, Bergstralh EJ, Slezak JM, Bostwick DG. Androgen receptor expression in prostatic intraepithelial neoplasia and cancer. J Urol 1999;161:1229–32. [PubMed: 10081875]

27. Koivisto PA, Helin HJ. Androgen receptor gene amplification increases tissue PSA protein expression in hormone-refractory prostate carcinoma. J Pathol 1999;189:219–23. [PubMed: 10547578]

28. Krijnen JL, Bogdanowicz JF, Seldenrijk CA, et al. The prognostic value of neuroendocrine differentiation in adenocarcinoma of the prostate in relation to progression of disease after endocrine therapy. J Urol 1997;158:171–4. [PubMed: 9186347]

29. di Sant'Agnese PA. Neuroendocrine differentiation in prostatic carcinoma: an update on recent developments. Ann Oncol 2001;12(Suppl 2):S135–40. [PubMed: 11762341]

30. Ray P, Wu AM, Gambhir SS. Optical bioluminescence and positron emission tomography imaging of a novel fusion reporter gene in tumor xenografts of living mice. Cancer Res 2003;63:1160–5. [PubMed: 12649169]

31. Pantuck AJ, Matherly J, Zisman A, et al. Optimizing prostate cancer suicide gene therapy using herpes simplex virus thymidine kinase active site variants. Hum Gene Ther 2002;13:777–89. [PubMed: 11975845]

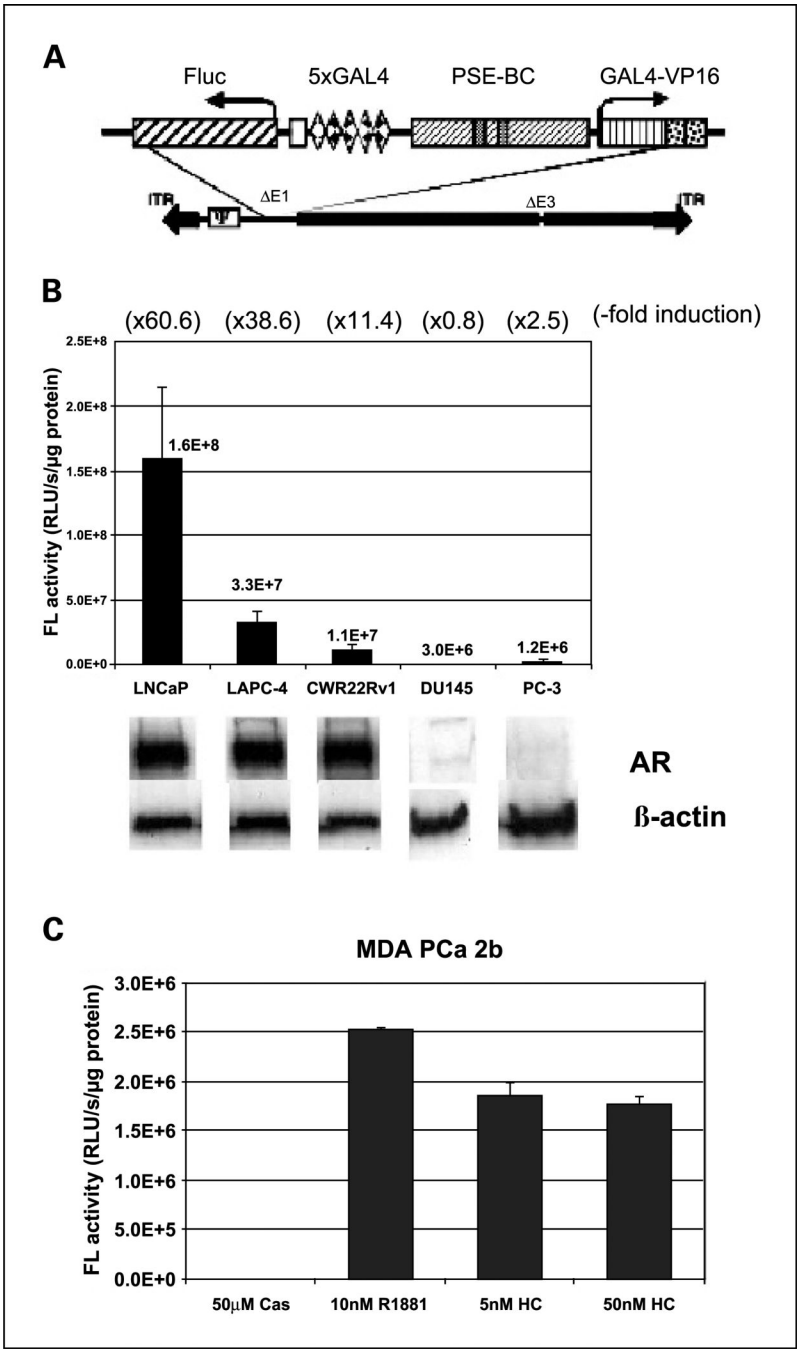

Fig. 1.

The activity of AdTSTA-FL and the induction with androgen in a panel of prostate cancer cell lines. *A*, schematic representation of the AdTSTA-FL. The two TSTA components of activator (*GAL4-VP16* driven by *PSE-BC*) and reporter (*Fluc* driven by *5xGAL4*) are inserted into E1 region of recombinant adenovirus. *B*, AdTSTA-FL activity on a panel of prostate cancer cell lines. The cell lysates were harvested 2 days after infection and subjected to FL activity and Western analysis with anti-AR antibody. Fold inductions calculated by the activity ratio with 10 nmol/L R1881 over 10 μmol/L casodex are indicated at the top in parentheses. The activity difference between the AR-positive cell lines and the AR-negative lines (*DU-145* and *PC-3*) is statistically significant ($P < 0.01$). *C*, AdTSTA-FL activity in MDA PCa 2b. The cells were

infected and incubated with 10 μmol/L casodex, 10 nmol/L R1881, and 5 and 50 nmol/L hydrocortisone.

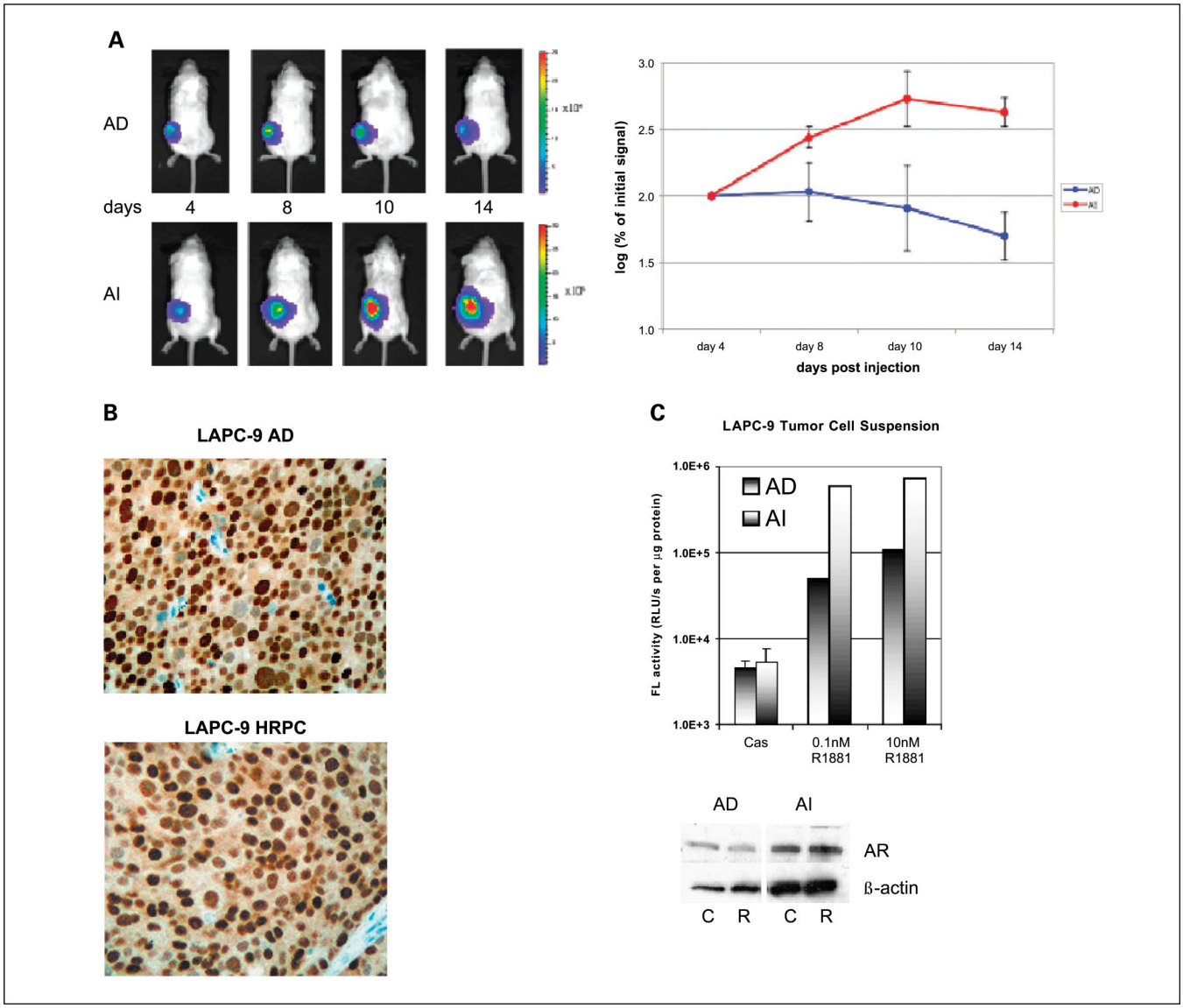

Fig. 2.

AdTSTA-FL – mediated activity *in vivo*. *A*, AdTSTA-FL – mediated optical signal in LAPC-9 AD and AI (HRPC) tumors. Ten million infectious units of virus were injected i.t. and imaged by optical CCD camera on the specified day postviral injection. Common logarithms of the percentages of the signal at day 4 of AD and AI tumors are plotted in the right panel. *B*, AR protein in LAPC-9 tumors. Paraffin-fixed, thin tumor sections were stained with anti-AR antibody. *C*, AdTSTA-FL activity in tumor cell suspension prepared from LAPC-9 AD and AI (HRPC) tumors. Tumor cell suspension was infected with AdTSTA-FL at MOI = 1 and incubated in the presence of 10 μmol/L casodex or 0.1 or 10 nmol/LR1881. The cell lysates were prepared after 2 days and subjected to FL assay and AR Western blot [10 μmol/L casodex (*C*); 10 nmol/LR1881 (*R*)]. The activity difference between AI and AD cells in the presence of R1881 was statistically significant ($P < 0.01$).

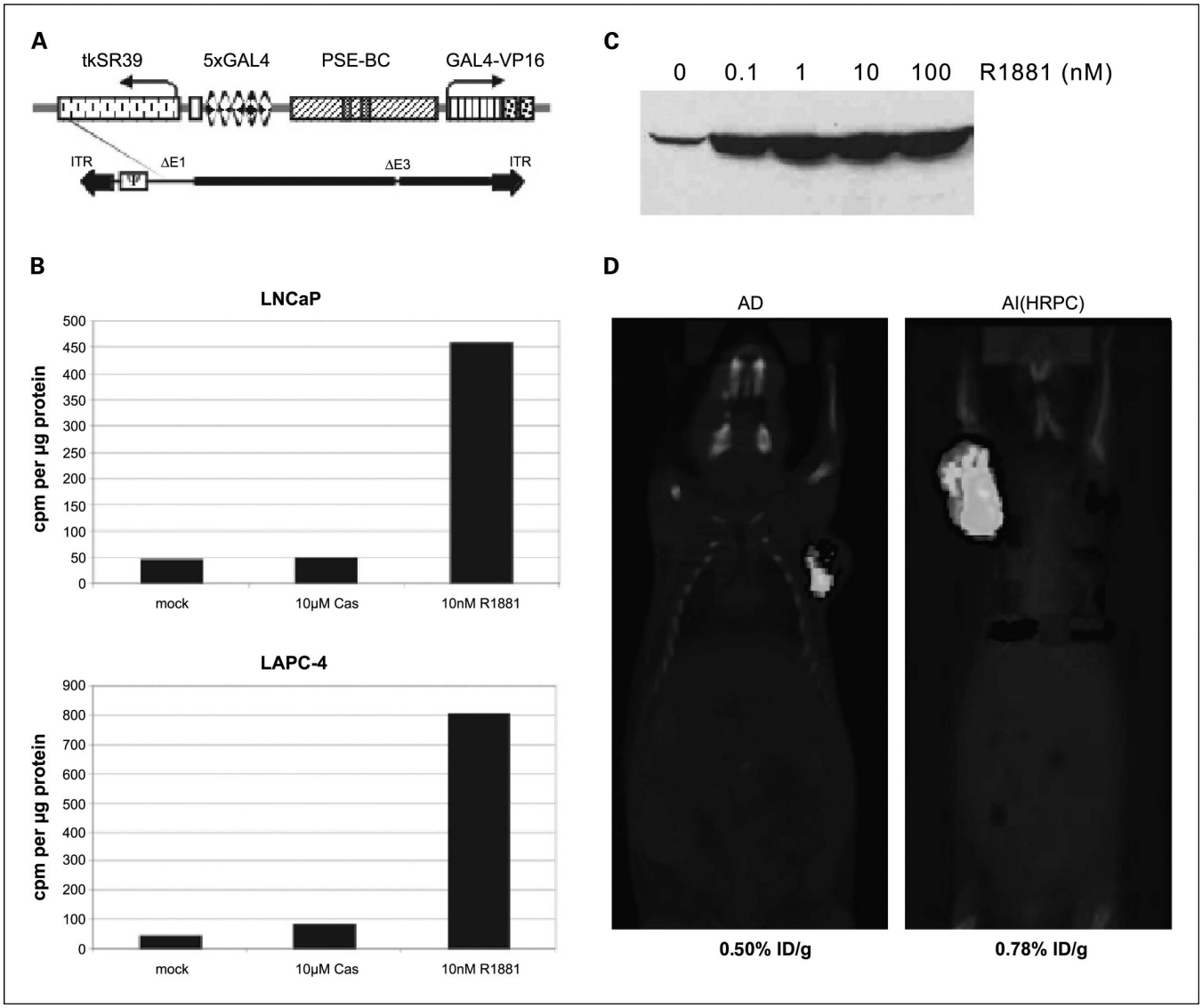

Fig. 3.

The activity of AdTSTA-sr39tk and its application in micro-PET. *A*, schematic representation of the AdTSTA-sr39tk. The *sr39tk* gene is a HSV-tk variant with higher affinity for acycloguanosines. *B*, AdTSTA-sr39tk activity in AD prostate cancer cell lines LNCaP and LAPC-4. The cells were infected with AdTSTA-sr39tk at MOI = 1 and harvested 2 days later. The cell lysates were subjected to thymidine kinase enzyme assay. Phosphorylated forms of [^{3}H]penciclovir were counted and plotted after normalization with total cellular protein. *C*, androgen regulation of expression from AdTSTA-sr39tk. LNCaP cells were infected with AdTSTA-sr39tk at MOI = 5 and incubated with 0 to 100 nmol/L R1881. Cells were lysed and subjected to Western analysis using anti-HSV-tk polyclonal antibody. *D*, combined micro-PET and micro-CT of LAPC-4 AD and AI tumor. AdTSTA-sr39tk (4×10^{9} infectious units) was injected to AD and AILAPC-4 tumors. One week later, [^{18}F]FHBG injected animals were anesthetized and scanned for micro-PET and micro-CT sequentially. The signal in the tumor was measured by percentage injected dose of substrate per gram of tissue (*%ID/g*) listed below the image.